RSC Advances

PAPER

View Article Online
View Journal | View Issue



Cite this: *RSC Adv.*, 2021, **11**, 16924

# Polyimides containing a novel bisbenzoxazole with high $T_g$ and low CTE

Haiquan Chen, Fengna Dai, Mengxia Wang, Chunhai Chen, Guangtao Qian* and Youhai Yu*

Received 20th March 2021
Accepted 28th April 2021

DOI: 10.1039/d1ra02218k

rsc.li/rsc-advances

A novel diamine named (2,2′-bibenzoxazole)-5,5′-diamine (DBOA) and derived polyimides (PIs) were successfully synthesized. The rigid, linear, symmetrical molecular structure and the strong charge transfer complex (CTC) were considered to be the reasons for the improved molecular packing and enhanced thermal properties of the polymers. These DBOA based PIs exhibited a higher glass transition temperature ($T_g$) and lower coefficient of thermal expansion (CTE) than traditional benzoxazole (BOA) based PIs. Meanwhile, the PI derived from DBOA and BPDA (3,3′,4,4′-biphenyltetracarboxylic dianhydride) exhibited high $T_g$ (395 °C) and low CTE (8.9 ppm per °C), and is expected to be applied in organic light-emitting diode (OLED) displays.



## 1. Introduction

With the development of flexible display devices, light and flexible polymer substrates are considered to be the most promising replacement for existing inorganic glass substrates. However, the manufacturing process of top emission-mode organic light-emitting diode (OLED) displays puts forward strict requirements on the thermal properties of polymers, including high glass transition temperature ($T_g$ > 350 °C) and low coefficient of thermal expansion (CTE < 10 ppm per °C).[1] As a type of special engineering polymer material, polyimide (PI) has been studied for flexible substrate due to excellent heat resistance and insulation.[2–4] For example, the commercially available PI films of Kapton H® (DuPont) and Upilex S® (Ube Industries) show high $T_g$ values (>350 °C). However, these films cannot meet the requirement of low CTE for multiple heating and cooling cycles in device manufacturing, and their high CTE (>20 ppm per °C) will cause significant expansion or contraction.

Recently, a class of benzimidazole (BI) based modified PIs has been widely discussed due to rigid rod-like structure and the intermolecular hydrogen bonding formed between the proton donors (N–H on imidazole) and proton acceptors (C=O on imide).[5–8] Intermolecular hydrogen bonding can further restrict the inter-segment mobility, promote spontaneous in-plane orientation and increase the packing density, thus improving the heat resistance and reducing the CTE of the polymers. However, the introduction of the BI unit will also bring high water absorption to the derived PIs, accelerate the degradation of the imide ring, destroy the electrical insulation, and shorten the service life of the product.[9] Hopefully, benzoxazole (BO) behaved rigidity and linearity comparable to BI without bringing high water absorption, so it is meaningful and referential to develop high performance BO based PIs.

In this study, a novel diamine containing bisbenzoxazole was synthesized, as shown in Fig. 1. High aromatic heterocyclic content and linearity are expected to contribute to more excellent thermal properties, including higher $T_g$ and lower CTE. Meanwhile, the amine group on the aromatic heterocyclic ring exhibited stronger nucleophilicity than phenyl ring,[10,11] increasing formation of CTCs and promoting aromatic packing. The DBOA based PIs were successfully prepared, and its physical properties were compared with the traditional BOA based PI.

## 2. Experiment

### 2.1 Materials

2-Amino-4-nitrophenol and methyl 2,2,2-trichloroacetimidate were purchased from Shanghai Energy Chemical Co., Ltd. 2-(4-Aminophenyl)benzoxazol-5-amine (BOA), 3,3′,4,4′-biphenyltetracarboxylic dianhydride (BPDA), 3,3,4,4-benzophenonetetracarboxylic dianhydride (BTDA) and 4,4′-oxydiphthalic anhydride (ODPA) were purchased from Tokyo Chemical Industry (Shanghai), dried in a vacuum oven at 150 °C for 24 h then to use. Acetic acid (HOAc, AR), triethylamine (TEA, AR), *N*,*N*-dimethylacetamide (DMAc, AR), palladium 10% on charcoal (water content 50–65%) and 80% hydrazine monohydrate and other reagents were purchased from Sinopharm Chemical Reagent Shanghai Co., Ltd. 1-Methyl-2-pyrrolidinone (NMP, electronic grade, 99.9%) was purchased from Beijing Innochem Technology Co., Ltd. Unless otherwise stated, all reagents and solvents were used directly without further purification or water removal.

*Center for Advanced Low-Dimension Materials, State Key Laboratory for Modification of Chemical Fibers and Polymer Materials, College of Material Science and Engineering, Donghua University, Shanghai 201620, P. R. China. E-mail: qgt@dhu.edu.cn; yuyouhai@dhu.edu.cn; Tel: +86-21-67798670*

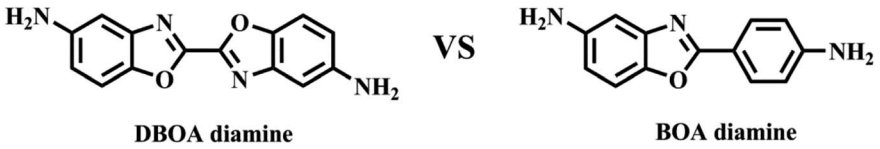


DBOA diamine BOA diamine

Fig. 1 Molecular structure of diamines.



### 2.2 Measurements

The proton nuclear magnetic resonance ($^1$H NMR) spectra of compound were recorded by a Bruker 400 AVANCE III spectrometer using DMSO-$d_6$ as the sample solvent. The geometry conformation optimization of monomer were based on density functional theory (DFT) with the B3LYP hybrid functional and [6-31G(d,p)] basis set on Gaussian 16. The inherent viscosities ($\eta_{inh}$) of poly(amic acid) (PAA) solution were performed on an Ubbelohde viscometer by configuring a dilution of 0.5 g dL$^{-1}$ with NMP and operating in a water bath thermostat at 25 °C. Fourier transform infrared (FT-IR) spectra were recorded on a Thermo Scientific Nicolet iS50 FT-IR spectrometer from 4000 to 400 cm$^{-1}$ by averaging 32 scans (KBr pellets for compound powders, film samples switching ATR accessory). Film densities ($\rho$) were performed on solid density analytical balance (XS204, Mettler Toledo, Shanghai, China). The packing coefficient ($K$) was estimated from following equation:[12]

$$K = \frac{v_{int}}{v_{true}} = \frac{N_A \sum \Delta V_i}{M/\rho}$$

where $N_A$ represents the Avogadro number, $\Delta V_i$ the volume increments of the atoms and atomic groups forming the repeating unit, $M$ the molecular weight of the repeating unit and $\rho$ the density of the polymer. The water absorption ($W_A$) of the PI films was calculated by the following equation:

$$W_A = \frac{W_b - W_a}{W_a} \times 100\%$$

where $W_a$ represents the quality of the sample film after being dried at 150 °C, $W_b$ the quality of the sample film after being immersed in deionized water at 25 °C for 24 h then removed surface water. Wide-angle X-ray diffractometry (WXRD) spectra were recorded by a Rigaku Denki D/MAX-2500 diffractometer with Cu K$\alpha$ ($\lambda = 1.54$ Å) radiation. Thermogravimetric analysis (TGA) of PI films was operated on Discovery TGA 550 Instrument (TA Instruments, USA) under a nitrogen flow rate of 25 mL min$^{-1}$ with a heating rate of 10 °C min$^{-1}$. Dynamic mechanical analysis (DMA) of PI films was operated on DMA Q800 (TA Instruments, USA) with a load frequency of 1 Hz and a heating rate of 5 °C min$^{-1}$ under nitrogen, defining the peak temperature of tan $\delta$ curve as glass transition temperature. The coefficient of thermal expansion (CTE) of the PI films were operated on a Q400 TMA (TA Instruments, USA) at a heating rate of 5 °C min$^{-1}$ under nitrogen with a preload of 0.1 N, calculating the CTE values of the temperature ranges of 50–250 °C. Mechanical properties were carried on an Instron 5966 testing apparatus with a crosshead speed of 5 mm min$^{-1}$, and tensile strength ($T_s$), tensile modulus ($T_m$) and elongation ($E_b$) were averaged from five parallel samples.

### 2.3 Synthesis of monomers

**5-Nitro-2-(trichloromethyl)-benzoxazole (1).** 2-Amino-4-nitrophenol (15.0 g, 97 mmol) and 150 mL acetic acid were poured into a three-necked round bottom flask equipped with mechanical stirring. When the mixture was cooled to 0–5 °C, methyl 2,2,2-trichloroethaneimidate (19.0 g, 108 mmol) was added dropwise, and reacted at room temperature for 12 h, accompanied by white precipitation. Finally, the reaction solution was poured into ice water (450 mL), washed repeatedly to remove acetic acid, and dried to obtain gray powder intermediate **1** (19.2 g, yield: 70.5%). $^1$H NMR (400 MHz, DMSO-$d_6$, ppm) $\delta = 8.22$ (d, 1H, $J = 12$ Hz), 8.52 (dd, 1H, $J = 2.4$, 2.4 Hz), 8.91 (d, 1H, $J = 2.0$ Hz). FTIR (KBr, $\nu$, cm$^{-1}$): 1688, 1592 ($\nu_{C=N}$ of oxazole); 1525, 1346 (–$NO_2$); 1280, 1058 (=C–O–C of oxazole). Anal. calcd for $C_8H_3Cl_3N_2O_3$: C, 34.14%; H, 1.07%; N, 9.95%. Found: C, 34.01%; H, 1.19%; N, 9.91%.

**5,5′-Dinitro-2,2′-bibenzoxazole (2).** 2-Amino-4-nitrophenol (8.2 g, 53 mmol), intermediate **1** (15.0 g, 53 mmol), 150 mL ethanol and triethylamine (10.7 g, 0.106 mol) were added to a 250 mL three-necked round bottom flask equipped with mechanical stirring and condensing reflux device, then the mixture was reacted at 80 °C for 72 h, accompanied by precipitation. The reaction solution was cooled to room temperature, filtered and continuously rinsed with ethanol and dried, recrystallization from DMAc solution gave a gray brown powder of dinitro intermediate **2** (3.6 g, yield: 20.7%). The dinitro intermediate **2** showed poor solubility in organic solution. FTIR (KBr, $\nu$, cm$^{-1}$): 1690, 1590 ($\nu_{C=N}$ of oxazole); 1524, 1348 (–$NO_2$); 1281, 1054 (=C–O–C of oxazole ring). Anal. calcd for $C_{14}H_6N_4O_6$: C, 51.55%; H, 1.85%; N, 17.17%. Found: C, 51.58%; H, 1.96%; N, 15.77%.

**(2,2′-Bibenzoxazole)-5,5′-diamine (DBOA).** Dinitro intermediate **2** (3.0 g, 9.2 mmol), Pd/C (0.3 g) and 30 mL 1,4-dioxane solution were added to a 250 mL three-necked round bottom flask equipped with magnetic stirring and condensing reflux device. When the mixture was heated to 80 °C, hydrazine hydrate (4.6 g, 92 mmol) was added dropwise with a dropping funnel, accompanied by a large number of bubbles. The mixture was refluxed at 80 °C for 6 h. The catalyst of Pd/C was removed by hot filtration and most of the solvent was removed by spin evaporation, then 100 mL of deionized water was poured into the concentrated solution, and the product was precipitated, then filtered and washed with water for 2–3 times, suction filtered and dried to give grey powder of DBOA (1.9 g, yield: 77.6%). $^1$H NMR (400 MHz, DMSO-$d_6$, ppm) $\delta =$ 5.30 (s, 4H), 6.83 (dd, 2H, $J = 1.6$, 1.2 Hz), 6.95 (d, 2H, $J = 1.6$ Hz), 7.54 (d, 2H, $J = 5.6$ Hz). FTIR (KBr, $\nu$, cm$^{-1}$): 3355, 3219 (–$NH_2$); 1681, 1586 ($\nu_{C=N}$ of oxazole); 1280, 1050 (=C–O–C of oxazole ring). Anal. calcd for $C_{14}H_{10}N_4O_2$: C, 63.15%; H, 3.79%; N, 21.04%. Found: C, 63.01%; H, 3.99%; N, 21.24%.

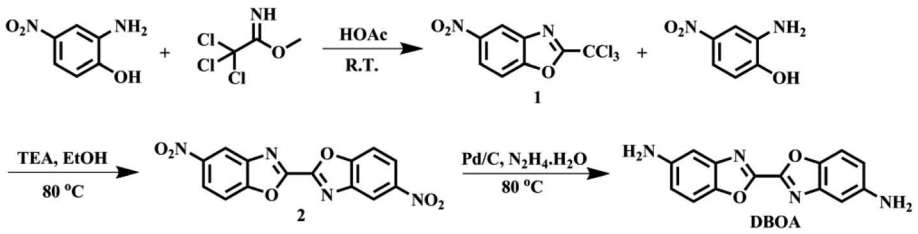


Scheme 1 Synthesis route of monomers.

### 2.4 Polymerization and film preparation

In this study, two-step thermal imidization method was used to prepare homopolyimide film. A typical synthetic route was as followed: DBOA (0.5000 g, 1.88 mmol), BPDA (0.5525 g, 1.88 mmol) and NMP solution (10 g) were added to a 50 mL three-necked round bottom flask equipped with mechanical stirring. The reaction mixture was stirred at room temperature for 12 h under dried nitrogen atmosphere. The final obtained PAA solution (9.5 wt%) was allowed to stand still to remove air bubbles in low temperature (0–5 °C). The obtained homogeneous and viscous PAA solution was cast on a flat and clean glass plate with a 400 μm depth blade and placed in an 80 °C oven for 12 h to remove most of the solvent, then heated at established imidization temperatures typically at 200 °C, 300 °C and 400 °C for 1 h at each temperature. After cooling to room temperature, the glass plate was put into deionized water, the PI film gradually peeled off, and dried in a 150 °C vacuum oven for 24 h.

## 3. Results and discussion

### 3.1 Diamine and polymer synthesis

The diamine of DBOA was prepared through a three-step reaction, as shown in Scheme 1, and the obtained monomers were characterized by $^1$H NMR (Fig. 2). All proton hydrogen can be well assigned on the $^1$H NMR spectra, and the proton peak of the amine group appeared at 5.30 ppm, indicating that the dinitro intermediate was successfully reduced to the target diamine DBOA. The $^1$H NMR spectrum of BOA was compared with DBOA. Different from the single chemical shift of proton hydrogen attached on amine in DBOA, the proton hydrogen attached on amine of BOA exhibited two types of chemical shifts due to different chemical environment, and the chemical shift of amine attached on BO was lower than phenyl ring, indicating that the amine attached on BO showed higher nucleophilicity than the amine attached on phenyl ring. In addition, the net charge distribution and spatial geometric conformation of BOA and DBOA were simulated by DFT (Fig. 3). The N atom of amines attached on BO showed higher net charges than the one attached to the phenyl ring, which also indicated the higher nucleophilicity of amine attached on BO than the one on phenyl ring. As a result, diamines with high nucleophilicity would accelerate the formation of CTCs. The spatial conformation of DBOA showed ideal linear center symmetry, and the dihedral angle of the two benzoxazole planes was 180°, suggesting the two small rigid planes formed a larger rigid coplanar plane.[8,13] This linear, flat and rod-like spatial structure will help us understand the molecular packing of polymers.

In this study, all PIs were prepared through two-step thermal imidization method by DBOA with commercial dianhydrides, including BPDA, BTDA, ODPA (Scheme 2). The obtained PIs showed excellent resistance to organic solubility, and PAA solutions exhibited ideal inherent viscosity, indicating high molecular weights.

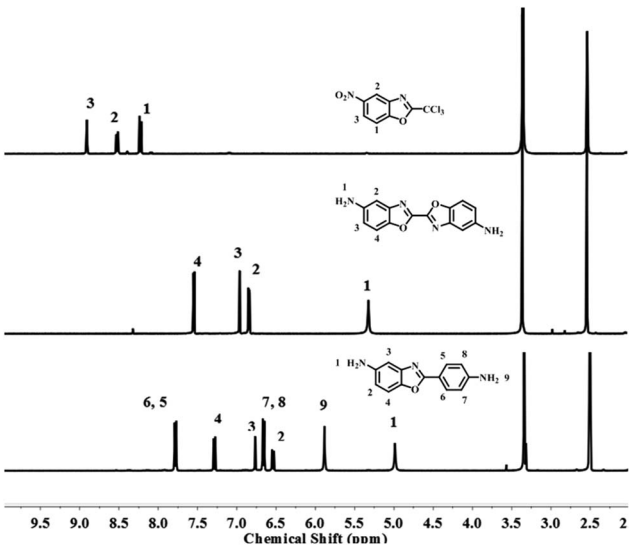


Fig. 2 $^1$H NMR spectra of monomers.

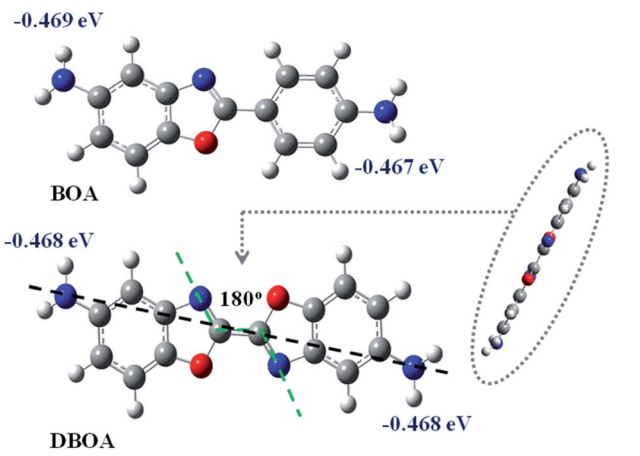


Fig. 3 Optimal conformation and net charge distribution of diamines by the DFT.

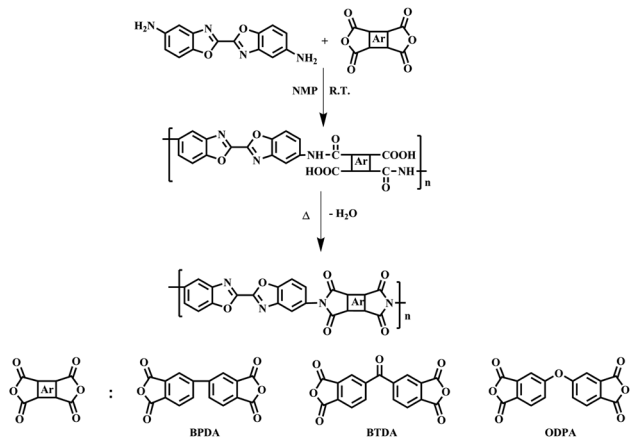


Scheme 2 Synthesis of PIs.

Furthermore, the structure of obtained PIs was characterized by FT-IR spectra, as shown in Fig. 4. The obtained novel PIs showed similar characteristic absorption peaks at approximately 1770 $cm^{-1}$, 1700 $cm^{-1}$ and 1362 $cm^{-1}$, which corresponded to asymmetric/symmetric stretching of C=O on cyclic imide, as well as stretching of C–N on cyclic imide, indicating the successful synthesis of cyclic imide rings.[1,14,15] The FT-IR spectra also showed the characteristic absorptions at 1250 $cm^{-1}$ (Ar–C–O asymmetric stretching) and 925 $cm^{-1}$ (O–C=N in-plane deformation),[16] suggesting that the BO unit has been successfully introduced into the main chains of PIs. Besides, N–H stretching peaks around 3250–3450 $cm^{-1}$ disappeared, indicating that precursor PAAs were successfully converted to the expected PIs.[15,17]

### 3.2 Molecular packing

The molecular packing of polymer is related to the molecular structure and intermolecular interactions. The novel double-rod bisbenzoxazole showed more rigid components, and the symmetrical, linear, flat structure was conducive to the orderly packing of molecules. In addition, the introduction of abundant aromatic heterocycles further promoted intermolecular interactions, including aromatic packing and CTCs. As shown in Table 1, the obtained PI films had densities ($\rho$) of 1.414–1.421 g $cm^{-3}$, which were higher than common aromatic polymers and PIs containing benzoazole units.[8] Meanwhile, the packing coefficient ($K$) was used to further evaluate the molecular packing, the obtained PIs showed $K$ values of 0.699–0.710, while the $K$ values of ordinary polymers were mostly ranged from 0.665 to 0.695,[8] which proved that the introduction of bisbenzoxazole to promote the intermolecular packing is feasible. The resulting PI films also exhibited low water absorption ($W_A$) of 1.30% to 1.85% also due to the close molecular packing, which were much lower than the reported

Table 1 Inherent viscosities, density, packing coefficient and water absorption of PIs

| PI | $\eta_{inh}$[a] (dL $g^{-1}$) | $\rho$ (g $cm^{-3}$) | $K$ | $W_A$ (%) |
|---|---|---|---|---|
| DBOA–BPDA | 1.18 | 1.421 | 0.710 | 1.30 |
| DBOA–BTDA | 1.07 | 1.420 | 0.700 | 1.79 |
| DBOA–ODPA | 1.10 | 1.414 | 0.699 | 1.85 |

[a] Obtained by PAA solutions.

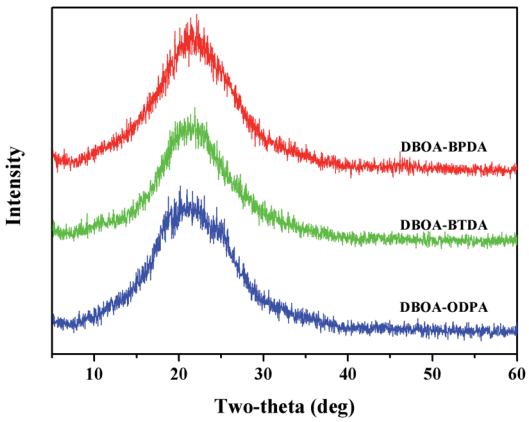


Fig. 5 The WXRD spectra of PI films.

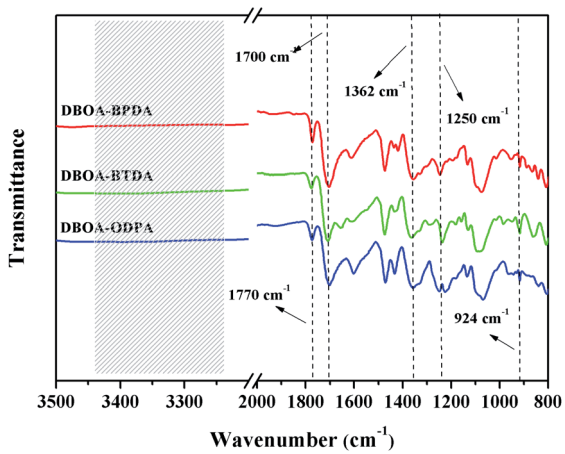


Fig. 4 The FT-IR spectra of PI films.

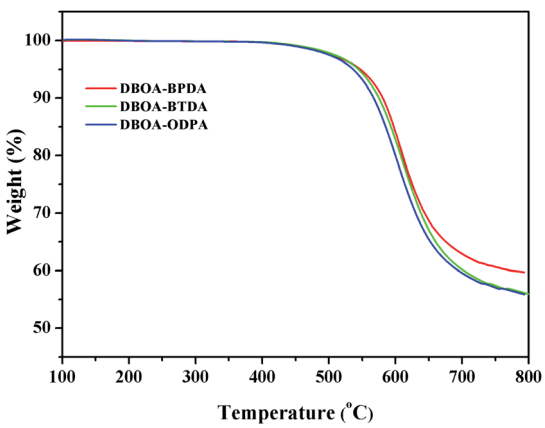


Fig. 6 The TGA curves of PI films.

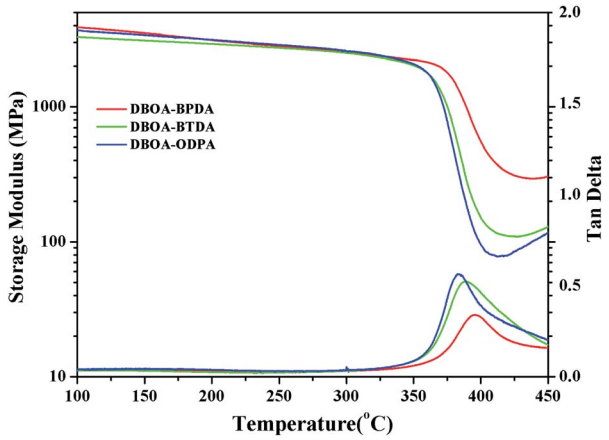


Fig. 7 The DMA curves of PI films.

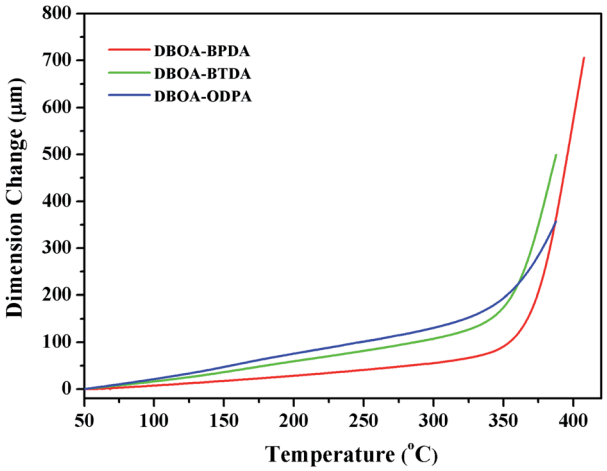


Fig. 8 The TMA curves of PI films.

BIA-based PIs.[16,18,19] In addition, wide-angle X-ray diffraction (WXRD) spectroscopy was used to characterize the microscopic morphology of the resulting PI films.[20] All spectra showed diffuse broad diffraction peaks without obvious splitting peaks (Fig. 5), indicating all PIs were basically amorphous. In detail, where $2\theta$ around 23° could be assigned to the interchain π–π packing order.[21,22]

### 3.3 Properties of polyimides

The thermal stability the resulting PIs was characterized by thermogravimetric analysis (TGA, Fig. 6), and dynamic thermomechanical analysis (DMA) was used to characterize the $T_g$ (Fig. 7), the results were summarized in Table 2. The obtained PIs showed outstanding heat resistance, the initial decomposition temperature was more than 400 °C, and the 5%, 10% weight loss temperatures under nitrogen were in the range of 549–557 °C ($T_{d5\%}$) and 578–588 °C ($T_{d10\%}$), which can meet the temperature of flexible substrate process ($T_{d5\%}$ > 500 °C).[1–3] Thanks to the fully aromatic molecular backbone, the strong conjugation and rich CTCs accelerated the heat conduction between the intra-segments and slowed down the degradation of the molecular chains.[8] The $T_g$ of polymers was affected by rigid and linear of molecular structure. For example, Jiao *et al.*[23] synthesized two non-linear isomeric diamines containing benzoxazole moieties, which effectively reduced the $T_g$ and improved melt processability of derived PIs. In this study, the double-rod bisbenzoxazole units strengthened the rigidity and linearity of the molecular backbone, effectively prevented the free rotation of the molecular chains, and inhibited intra-segments mobility. Meanwhile, the CTC enhanced by the bisbenzoxazole aromatic heterocycle further strengthened the intermolecular interaction, restricted inter-segments mobility, promoted the molecular effective packing, resulting in high $T_g$ values ranged from 382 to 395 °C, which were much higher than the reported PI of BOA–BPDA.[24] In addition, when the testing temperature were close to $T_g$ values, the storage modulus of such PIs decreased sharply due to the transition of polymer from glassy state to high elastic state and the molecular chains can move freely. Interestingly, testing temperature continued to rise, the storage modulus rebounded. In this study, when the temperature were higher than the $T_g$, the molecular chains spontaneously undergone in-plane orientation under intermolecular interactions, and the rigid and linear bisbenzoxazole units induced liquid crystal behavior,[25] promoted the local ordering of the molecular chains, resulting in the increase of the storage modulus.

The static thermomechanical analysis was used to characterize the dimensional stability of the obtained PI films, and the CTE values were determined by the TMA method (Fig. 8). The obtained PI films showed low CTE values ranged from 8.9 to 20.6 ppm per °C (Table 3), which were much lower than the commercially available PIs (30–50 ppm per °C).[26] In particular, DBOA–BPDA showed a ultra-low CTE value of 8.9 ppm per °C and a high $T_g$ of 395 °C, which can meet the demands of OLED flexible substrate. The CTE of polymers is considered to be related to molecular packing and orientation.[27–29] The rigid, linear and flat bisbenzoxazole units restricted the free rotation of the segments and promoted the aromatic packing. Moreover,

Table 2 Thermal properties of PIs[a]

| PIs | $T_g$ (°C) | $T_{d5\%}$ (°C) | $T_{d10\%}$ (°C) | CTE (ppm per °C) |
|---|---|---|---|---|
| DBOA–BPDA | 395 | 557 | 588 | 8.9 |
| DBOA–BTDA | 388 | 554 | 582 | 16.4 |
| DBOA–ODPA | 382 | 549 | 578 | 20.6 |
| BOA–BPDA[24] | 302 | | | |

[a] $T_{d5}$, $T_{d10}$: temperature of 5%, 10% weight loss.

Table 3 Mechanical properties of PI films

| PIs | Tensile strength/MPa | Tensile modulus/GPa | Elongation at break/% |
|---|---|---|---|
| DBOA–BPDA | 259 ± 3 | 5.2 ± 0.1 | 3.4 ± 0.2 |
| DBOA–BTDA | 229 ± 3 | 5.0 ± 0.3 | 4.8 ± 0.2 |
| DBOA–ODPA | 223 ± 4 | 4.9 ± 0.2 | 4.9 ± 0.3 |

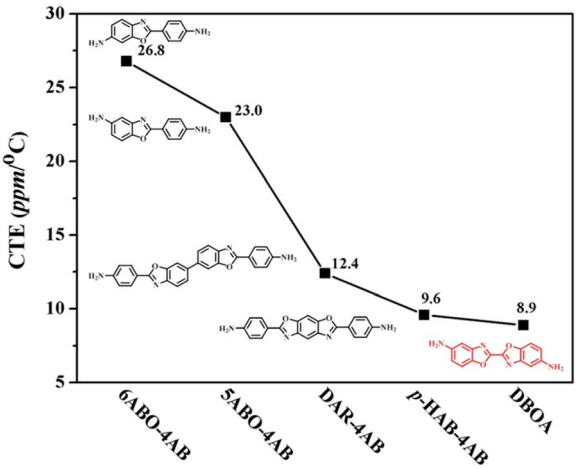


Fig. 9 CTE values of PIs derived from different benzoxazole based diamines and same BPDA dianhydride.[1]

during the thermal imidization process, the enhanced intermolecular CTCs induced the spontaneous in-plane orientation of the molecules. The reported CTE values of PIs derived from BOA based diamines[1] and BPDA were summarized in Fig. 9. It can be clearly seen that bisbenzoxazole based diamines (DAR-4AB, *p*-HAB-4AB, DBOA) had more potential to reduce the CTE of derived PIs than single-benzoxazole based diamines (6ABO-4AB, 5ABO-4AB). The DBOA based PI exhibited a slightly lower CTE value than DAR-4AB and *p*-HAB-4AB, which may be due to the stronger nucleophilicity of the diamines on the benzoxazole. In addition, DBOA–BTDA and DBOA–ODPA showed higher CTE values than DBOA–BPDA, which was due to the flexible ether bond and carbonyl weakened the rigidity and linearity of the molecular chains and destroyed the molecular effective packing. Nevertheless, they also showed lower CTE values than PIs of 6ABO-4AB-BPDA and 5ABO-4AB-BPDA, thus showing the potential of DBOA in reducing the CTE of polymers.

The mechanical properties of the resulting PI films were obtained by tensile testing, as shown in the Fig. 10, and summarized in Table 3. The films exhibited high tensile strength of 223–259 MPa, tensile modulus of 4.9–5.2 GPa and elongation at break of 3.4–4.9%. Similar to the thermal properties, DBOA–BPDA with more rigid molecular backbone and higher packing density exhibited higher tensile strength and modulus. However, too stiff molecular chains tended to cause brittle fracture of the film, while the introduction of flexible units can improve the elongation at break of the film, such as DBOA–BTDA and DBOA–ODPA. Nevertheless, this series of PI films were still expected to be used as flexible substrate materials with the tensile strength exceeding 100 MPa and the initial modulus for 2 GPa.[8]

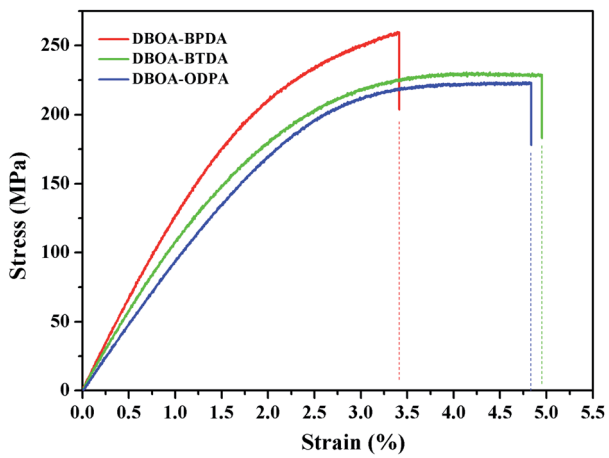


Fig. 10 The strain–stress curves of PI films.

## 4. Conclusions

In summary, novel bisbenzoxazole based PIs with high $T_g$ and low CTE were successfully prepared. The rigid, linear, symmetrical molecular structure, as well as the rich CTCs caused by the strong nucleophilicity of aromatic diamines were considered to be the reasons for the improvement of thermal and mechanical properties of the polymers. In addition, DBOA–BPDA showed the highest $T_g$ (395 °C) and the lowest CTE (8.9 ppm per °C) in the obtained PIs, meeting the requirements of flexible substrate for OLED displays. The novel DBOA diamine can be used as a candidate modified monomer to prepare high-performance PIs with high $T_g$ and low CTE, which also provides a reference for preparing flexible substrate polymer materials.

## Conflicts of interest

There are no conflicts to declare.

## Acknowledgements

This work was supported by Research Startup Program of Donghua University (285-07-005702) and the Key-Area Research and Development Program of Guangdong Province (2020B010182002). We thank Dr Lei Liu and Dr Li Wei for their help in the measurement and characterization of the paper.

## References

1 M. Hasegawa, Y. Hoshino, N. Katsura and J. Ishii, *Polymer*, 2017, **111**, 91–102.
2 X. Gao, L. Lin, Y. Liu and X. Huang, *J. Disp. Technol.*, 2015, **11**, 666–669.
3 J. Lewis, *Mater. Today*, 2006, **9**, 38–45.
4 D. J. Liaw, K. L. Wang, Y. C. Huang, K. R. Lee, J. Y. Lai and C. S. Ha, *Prog. Polym. Sci.*, 2012, **37**, 907–974.
5 L. Luo, J. Zhang, J. Huang, Y. Feng, C. Peng, X. Wang and X. Liu, *J. Appl. Polym. Sci.*, 2016, **133**, 44000–44007.
6 Y. Feng, L. B. Luo, J. Huang, K. Li, B. Li, H. Wang and X. Liu, *J. Appl. Polym. Sci.*, 2016, **133**, 43677–43686.
7 J. Dong, C. Yin, Z. Zhang, X. Wang, H. Li and Q. Zhang, *Macromol. Mater. Eng.*, 2014, **299**, 1170–1179.
8 M. Lian, X. Lu and Q. Lu, *Macromolecules*, 2018, **51**, 10127–10135.

9 L. Li, N. Bowler, P. R. Hondred and M. R. Kessler, *IEEE Trans. Dielectr. Electr. Insul.*, 2012, **18**, 1955–1962.
10 L. Luo, Y. Dai, Y. Yuan, X. Wang and X. Liu, *Macromol. Rapid Commun.*, 2017, **38**, 1700404–1700408.
11 L. Luo, Y. Zheng, J. Huang, K. Li, H. Wang, Y. Feng, X. Wang and X. Liu, *J. Appl. Polym. Sci.*, 2015, **132**, 42001–42009.
12 G. L. Slonimskii, A. A. Askadskii and A. I. Kitaigorodski, *Polym. Sci.*, 1970, **3**, 494–512.
13 J. L. Yan, Z. Wang, L. X. Gao and M. X. Ding, *Macromolecules*, 2006, **39**, 7555–7560.
14 M. Hasegawa, *J. Polym. Sci., Part B: Polym. Phys.*, 1993, **31**, 1617–1625.
15 Y. K. Xu, M. S. Zhan and K. Wang, *J. Polym. Sci., Part B: Polym. Phys.*, 2004, **42**, 2490–2501.
16 Y. Zhuang, X. Liu and Y. Gu, *Polym. Chem.*, 2012, **3**, 1517–1525.
17 Y. Chen and Q. Zhang, *J. Polym. Res.*, 2015, **22**, 78–86.
18 X. Yu, W. Liang, J. Cao and D. Wu, *Polymers*, 2017, **9**, 451–469.
19 G. Qian, F. Dai, H. Chen, M. Wang, M. Hu, C. Chen and Y. Yu, *RSC Adv.*, 2021, **11**, 3770–3776.
20 Y. Obata, K. Okuyama and S. Kurihara, *Macromolecules*, 1995, **28**, 1547–1551.
21 W. Chen, W. Chen, B. Zhang, S. Yang and C. Liu, *Polymer*, 2017, **109**, 205–215.
22 S. Wang, H. Zhou, G. Dang and C. Chen, *J. Polym. Sci., Part A: Polym. Chem.*, 2009, **47**, 2024–2031.
23 Y. Jiao, G. Chen, N. Mushtaq, H. Zhou, X. Chen, Y. Li and X. Fang, *Polym. Chem.*, 2020, **11**, 1937–1946.
24 C. Yin, J. Dong, D. Zhang, J. Lin and Q. Zhang, *Eur. Polym. J.*, 2015, **67**, 88–98.
25 M. A. Ali, H. Shimosegawa, A. Nag, K. Takada and T. Kaneko, *J. Polym. Res.*, 2017, **24**, 214–220.
26 S. urRehman, G. Song, H. Jia, H. Zhou, X. Zhao, G. Dang and C. Chen, *J. Appl. Polym. Sci.*, 2013, **129**, 2561–2570.
27 J. Ishii, N. Shimizu, N. Ishihara, Y. Ikeda, N. Sensui, T. Matano and M. Hasegawa, *Eur. Polym. J.*, 2010, **46**, 69–80.
28 S. Ebisawa, J. Ishii, M. Sato, L. Vladimirov and M. Hasegawa, *Eur. Polym. J.*, 2010, **46**, 283–297.
29 M. Hasegawa, T. Matano, Y. Shindo and T. Sugimura, *Macromolecules*, 1996, **29**, 7897–7909.